Selective hydrogenation of biomass derived substrates using ionic liquid-stabilized ruthenium nanoparticles†

Jennifer Julis,[a] Markus Hölscher[a] and Walter Leitner*[a,b]

Received 29th March 2010, Accepted 2nd June 2010
DOI: 10.1039/c004751a

Ionic liquid-stabilized ruthenium nanoparticles with an average size between 2–3 nm are very active catalysts for the hydrogenation of biomass derived substrates. Their catalytic performance complements that of classic homogeneous and heterogeneous ruthenium catalysts.

Biomass-derived substrates are receiving increasing interest as a part of a sustainable supply chain to chemical products and transportation fuels.[1] Carbohydrates constitute the largest fraction of terrestrial biogenic carbon sources. They can be converted into various platform molecules from which molecular diversity can be created through de- and re-functionalization steps. Among these central intermediates are 5-hydroxymethylfurfural (HMF) and furfural, which are accessible from hexoses and pentoses, respectively.[1,2] Further modification of these structures is possible by the incorporation of additional building blocks, for example through aldol condensation (Scheme 1).[3]

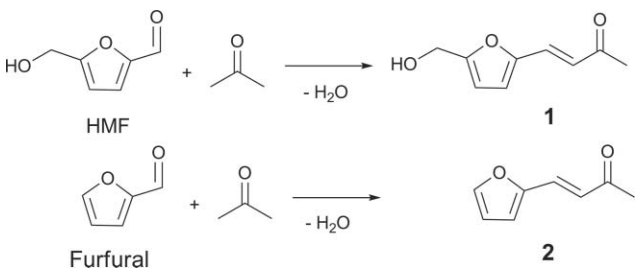

Scheme 1 Aldol-condensation of biomass-derived furfuryl derivates.

Selective hydrogenation of primary products **1** and **2** gives access to a range of increasingly saturated structures. Deep hydrogenation to the corresponding alkanes has been achieved by heterogeneously catalyzed reactions for both furfuryl derivates[3,4] and proposed as a selective route to individual linear alkanes. The intermediate hydrogenation products are also of interest, as they offer various options for further derivatization depending on the remaining functionalities (aromatic, olefinic, C=O, C–OH).

Scheme 2 shows all possible hydrogenation products that have not been deoxygenated, highlighting the challenge for the development of selective catalysts and processes to control their formation.

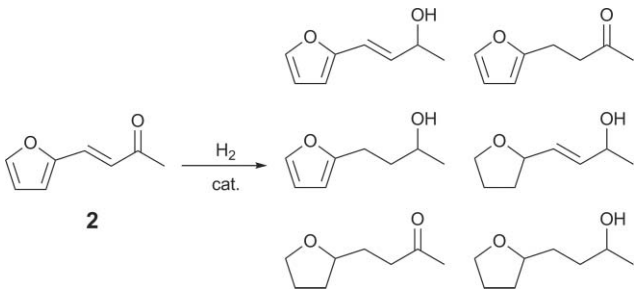

Scheme 2 Possible partial hydrogenation products derived from **2**.

Ionic liquid (IL)-stabilized metal nanoparticles are interesting new catalyst materials for hydrogenation and other applications.[5] For example, Dupont and co-workers prepared well-dispersed transition metal nanoparticles with narrow size distribution in a variety of imidazolium-based ILs, which showed very interesting activities in the hydrogenation of olefins and aromatic compounds like acetophenone.[6] Recently, we reported on the synthesis of rhodium nanoparticles in carbon dioxide induced ionic liquids, which were selective and active catalysts for the hydrogenation of C=C double bonds.[7] The specific properties of IL-stabilized metal nanoparticles place them at the interface between heterogeneous and homogeneous catalysts. On the one hand, IL-stabilized nanoparticles can form homogeneous dispersions avoiding mass transfer limitations. On the other hand, their active site is an ensemble of metal atoms rather than a single metal center and their nanoscale size often allows an efficient separation from the product.[8] The IL is not only a stabilizer, but often shows a strong influence on the catalytic properties similar to ligand control.[5]

Herein, we report on the synthesis and characterization of various IL-stabilized Ru-nanoparticle catalysts (Ru@IL) and their use for selective hydrogenation of the biomass-derived 4-(2-furyl)-3-butene-2-one **2** and related substrates. The size of the nanoparticles, their catalytic activity and selectivity can be controlled by variation of the IL. The novel catalyst systems are highly active and therefore excellent catalysts for the hydrogenation of C=O and C=C bonds, as well as for heteroaromatic systems. Moreover, they show interesting selectivities, which differ from classic homogeneous and heterogeneous Ru-catalysts.

[a]*Institute of Technical and Macromolecular Chemistry, RWTH Aachen, Worringerweg 1, 52074, Aachen, Germany.*
E-mail: leitner@itmc.rwth-aachen.de; Fax: (49) 0241-8022177;
Tel: (49) 0241-8026481
[b]*Max-Planck-Institut für Kohelnforschung, 45470 Mülheim an der Ruhr.*
† Electronic Supplementary Information (ESI) available: characterization of nanoparticles and products. See DOI: 10.1039/c004751a

Results and discussion

Synthesis and characterization

Metal nanoparticles are thermodynamically unstable and must be stabilized in solution to prevent agglomeration.[9] Stabilization can be achieved by steric and/or electronic shielding and ILs have been shown to combine both modes of action.[5,6,9,10] ILs often bind less strongly to the metal surface than other stabilizing agents, resulting in nanoparticles with high catalytic activity.

IL-stabilized transition metal nanoparticles can be easily generated by controlled decomposition of organometallic compounds or the reduction of transition metal compounds.[8] The ruthenium nanoparticles for this study were synthesized by reduction of bis(methylallyl)(1,5-cyclooctadiene) ruthenium(II) suspended in the IL at a metal loading of 2.5 wt% at 60 °C and 60 bar hydrogen pressure. As imidazolium based ILs have proven to be suitable for the stabilization of nanoparticles, imidazolium based ILs differing in the nature of the anion, the chain length or the substituent at the C2-position were used (Scheme 3). We varied the alkyl chain length to modulate the polarity and the substituents at C2-position to change the coordination ability. A set of anions differing in their nucleophilicity and coordination strength was chosen, as these factors are expected to influence the stability of nanoparticles.[5] The colours of the nanoparticle solutions ranged from dark brown to black. Except for the particle solutions synthesized in [EMMIM][BTA] and [EMIM][Br], no precipitate could be observed.

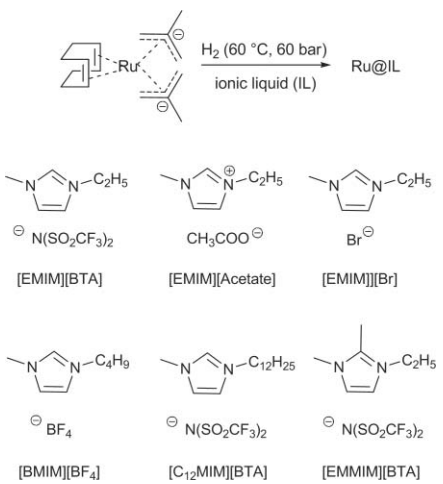

Scheme 3 Synthesis of ruthenium nanoparticles and imidazolium-based ILs used in this study.

The IL-stabilized ruthenium nanoparticles were characterized by transmission electron microscopy (TEM) (Fig. 1). The TEM image showed the formation of nearly monodispersed Ru@[C_{12}MIM][BTA] with an average diameter of 2.7 nm. The other particle systems also have narrow size distributions with average diameters between 2–3 nm. (Table 1).

Entry 1 shows that [EMMIM][BTA] is not suitable for the stabilization of nanoparticles, as primary particles with sizes in the range of 100–200 nm were formed. This is likely to result from the C2-position of the imidazolium ring being blocked, preventing the formation of surface attached carbene species, which has been reported to be an important factor for the

Table 1 Size of ruthenium nanoparticles in IL according to TEM analysis [a]

	Ionic liquid		
Entry	Cation	Anion	Size/nm
1	[EMMIM]	[BTA]	agglomerate
2	[C_{12}MIM]	[BTA]	2.7 ± 0.2
3	[EMIM]	[BTA]	2.4 ± 0.2
4	[EMIM]	[Br]	2.5 ± 0.5 and agglomerate
5	[EMIM]	[Acetate]	2.3 ± 0.2
6	[BMIM]	[BF_4]	2.0 ± 0.2

[a] Reaction conditions: 2.5 wt% Ru in IL, 60 °C, 60 bar H_2, 2 h.

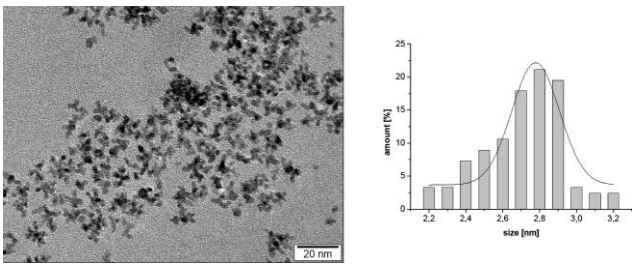

Fig. 1 TEM image of Ru nanoparticles prepared in [C_{12}MIM][BTA] (left) and resulting size distribution for 100 particles (right).

stabilization of Ir(0) nanoparticles.[11] With the exception of [EMIM][Br], which led to partial agglomeration, all other ILs are able to stabilize the ruthenium particles effectively. Increased chain length in the imidazolium cation and the variation of anions had no major influence on the particle size.

The system Ru@[C_{12}MIM][BTA] was further characterized by X-ray diffraction (XRD). For the XRD analysis, the nanoparticles were centrifuged, washed with acetone and dried under reduced pressure. The XRD pattern of the isolated material confirmed the formation of crystalline Ru^0. Using the Scherrer equation the mean diameter of these nanoparticles was determined to be 2.6 nm, which is in good agreement with the result of the TEM analysis.

Catalytic hydrogenation

The catalytic properties of the synthesized nanoparticles were investigated using **2** as a prototypical substrate. The hydrogenation reactions were carried out in a 10 mL stainless-steel reactor using the nanoparticle solutions directly without any additional solvents.

All nanoparticle systems were active in the hydrogenation of **2** with conversions of more than 99% after 2 h reaction time at 120 °C and 120 bar hydrogen pressure. However, product distributions differed significantly depending on the IL (Scheme 4, Table 2).

The product distribution reflects both activity and selectivity and provides an insight into the reactivity towards the different functional groups. All catalytic systems hydrogenate the C=C bond preferentially and with high rates. The [EMMIM][BTA] system forms selectively products **4** and **6**. Therefore, the hydrogenation of the aromatic ring is preferred over the hydrogenation of the C=O bond. This selectivity is typical for heterogeneous ruthenium catalysts indicating that the reduction occurs on an ensemble of ruthenium sites rather than a single ruthenium

Table 2 Hydrogenation of 4-(2-furyl)-3-butene-2-one **2** using Ru@IL catalysts

	Ionic liquid		Product distribution (%)				
Entry	Cation	Anion	(**3**)	(**4**)	(**5**)	(**6**)	Other
1	[EMMIM]	[BTA]	—	**47.5**	0.4	**45.9**	6.2
2	[C12MIM]	[BTA]	—	0.8	0.9	**94.2**	4.3
3	[EMIM]	[BTA]	0.1	0.5	0.9	**89.4**	8.1
4	[EMIM]	[Br]	**66.6**	31.0	1.9	0.5	—
5	[EMIM]	[Acetate]	**27.9**	14.6	**34.7**	19.6	3.1
6	[BMIM]	[BF_4]	0.3	28.0	0.4	**63.2**	8.1

2 h, 120 °C 120 bar; c(Ru) = 0.05 mol L^{-1}, Ru/substrate ratio 1 : 100, conversion >99%; other: unidentified by-products, including butyl-THF; bold numbers indicate the main products.

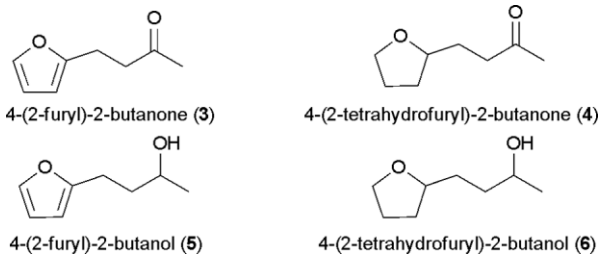

Scheme 4 Main hydrogenation products obtained from hydrogenation of **2** using Ru@IL catalysts.

center. The same is true for [EMIM][Br], which shows no significant activity for the C=O hydrogenation at all (entry 4). [EMIM][BF_4] and in particular BTA-based ILs with free C2-position form the most active systems leading to high to excellent selectivity for the saturated alcohol **6**. In contrast, [EMIM][Acetate] lead to a broad product mixture. The results show that control of selectivity by variation of IL is possible. The alkyl chain length in the imidazolium cation has only a minor influence on the selectivity of the catalytic system (entries 2 and 3). The selectivity is influenced much more by the anion of the ionic liquid (entries 3, 4, 5 and 6).

As Ru@[C_{12}MIM][BTA] exhibits the most promising results, the catalytic system was applied in the hydrogenation of other oxygenated substrates **7**, **1** and **10** (Table 3). After 2 h full conversion was achieved for all substrates. In all cases complete

Table 3 Hydrogenation of other substrates

Substrate	Product	Yield (%)
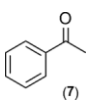 (**7**)	 (**8**)	99
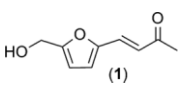 (**1**)	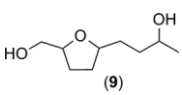 (**9**)	95
 (**10**)	 (**11**)	99

Ru@[C_{12}MIM][BTA], 2 h, 120 °C 120 bar; c(Ru) = 0.05 mol L^{-1}, Ru-substrate-ratio 1 : 100.

hydrogenation of all double bonds and also of the aromatic ring in **7** was observed, but oxygen functionalities remained intact. Thus, Ru@IL are promising catalytic systems for the selective hydrogenation of biomass based materials containing various functional groups like C=C, C=O, aromatic and heteroaromatic systems.[12] As mentioned before, Ru@[C_{12}MIM][BTA] showed the most promising stability and activity. Therefore, we analysed this system in more detail.

Recycling

The separation and recycling of the catalytic system Ru@[C_{12}MIM][BTA] was investigated for the hydrogenation reaction of **2**. After the first reaction run the products were extracted with supercritical carbon dioxide ($scCO_2$) from the reaction mixture at 40 °C and 150 bar CO_2.[13] To the remaining catalytic solution a fresh portion of substrate was added and the autoclave was pressurized again with H_2.

Fig. 2 shows that the recovered catalytic solution could be reused several times without any significant loss in conversion (>99% in all runs) and selectivity towards product **6**. The successful recycling is in good agreement with TEM analysis of the ruthenium nanoparticles after the reaction. No agglomeration of particles and only slight change in size and distribution were observed (Fig. 3).

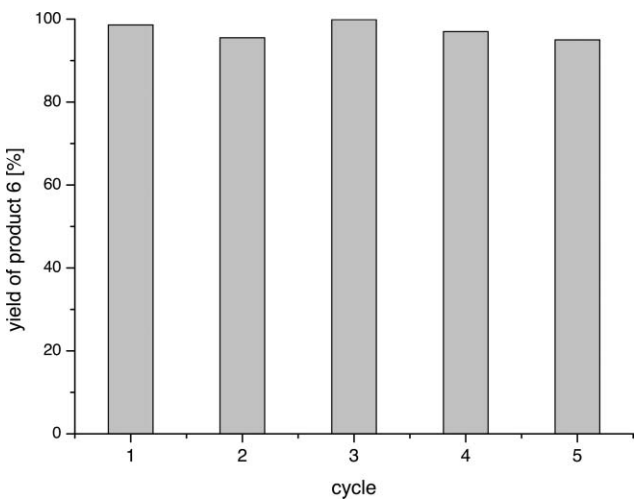

Fig. 2 Yield of product **6** in recycling experiment with Ru@[C_{12}MIM][BTA].

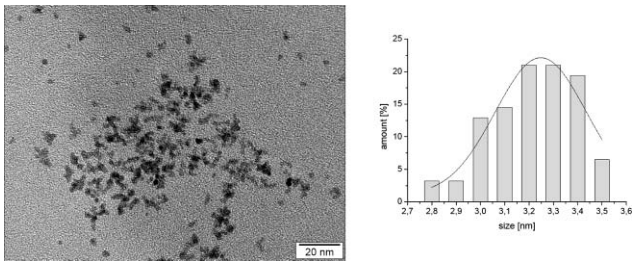

Fig. 3 TEM image of Ru@[C_{12}MIM][BTA] (left) and size distribution for 100 particles (right) recycled from $scCO_2$ extraction after catalysis.

To examine contamination of the extracted product, the ruthenium content was determined using inductively-coupled-plasma mass-spectrometry (ICP-MS). The leaching was determined to be <5 ppm indicating only negligible loss of the ruthenium catalyst by extraction with $scCO_2$. Thus, extraction with $scCO_2$ as a non-conventional solvent offers the possibility for product isolation and efficient catalyst separation and avoids the use of any volatile organic solvents.

Monitoring the course of reaction

To gain deeper insight into the hydrogenation of the various functional groups in the substrate, the reaction was monitored by sampling under reaction conditions (Fig. 4 and Fig. 5). Milder

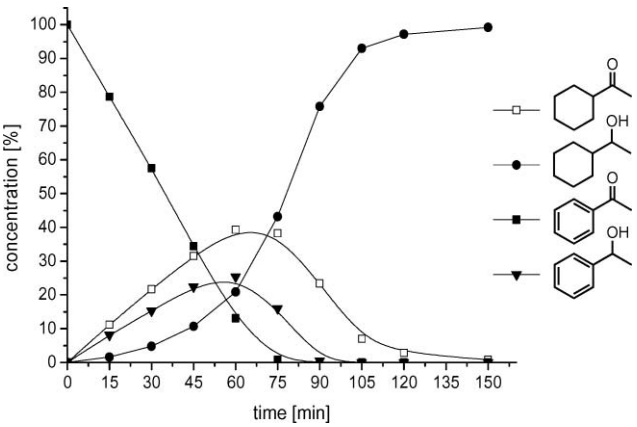

Fig. 4 Conversion-time profile for the hydrogenation of acetophenone **7** using Ru@[C_{12}MIM][BTA].

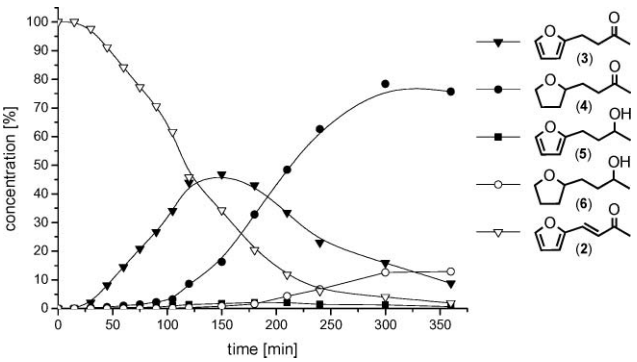

Fig. 5 Conversion-time profile for the hydrogenation of 4-(2-furyl)-3-butene-2-one **2** using Ru@[C_{12}MIM][BTA].

Table 4 Catalytic performance of Ru@[C_{12}MIM][BTA], [RuHCl-(PPh_3)$_3$] and ruthenium on alumina

		Product distribution (%)				
Entry	Catalyst	(**3**)	(**4**)	(**5**)	(**6**)	Others
1*a*	Ru@[C_{12}MIM][BTA]	0.1	80.8	—	16.0	2.9
1*b*		—	0.8	0.9	94.2	4.3
2*a*	RuHCl(PPh_3)$_3$	87.3	1.0	10.1	—	1.1
2*b*		65.0	16.7	15.3	0.9	2.1
3*a*	Ru on alumina	68.1	23.0	5.2	2.9	0.6
3*b*		—	0.6	0.2	97.6	1.6

2 h, c(Ru) = 0.05 mol L^{-1} in [C_{12}MIM][BTA], Ru-substrate ratio 1 : 100, conv. of **2** >99%; *a*: 60 °C, 60 bar H_2; *b*: 120 °C, 120 bar H_2.

reaction conditions (60 °C, 60 bar H_2) were applied to decelerate the reaction rate for a detailed analysis.

No distinct differentiation of the functional groups was observed in the hydrogenation of **7**. 1-Cyclohexylethanone and 1-phenylethanol were formed at similar rates indicating that the reactivity of the aromatic ring and the carbonyl group differ only slightly. This is consistent with the observations of Fonseca *et al.*, who monitored the hydrogenation of acetophenone in the presence of IL-stabilized iridium nanoparticles and observed a similar reactivity pattern.[14]

In contrast, the hydrogenation of **2** over Ru@[C_{12}MIM][BTA] occurred as a consecutive reaction (Fig. 5). At first the C=C double bond of the substrate was hydrogenated, followed by the hydrogenation of the heteroaromatic ring. Finally, the reduction of the carbonyl group took place, which was very slow under the mild reaction conditions. This distinct selectivity of Ru@[C_{12}MIM][BTA] in the hydrogenation of different functional groups allows to access selectively either product **4** or **6** as the main product of the reaction.

Comparison to other catalytic systems

The catalytic performance of Ru@[C_{12}MIM][BTA] in the hydrogenation of **2** was compared with the catalytic behaviour of classic heterogeneous and homogeneous ruthenium catalysts. The reference experiments were carried out with ruthenium on alumina as the heterogeneous catalyst and [RuHCl(PPh_3)$_3$] as the homogeneous catalyst under identical reaction conditions (Table 4).

Depending on the reaction conditions Ru@[C_{12}MIM][BTA] allows production of either product **4** or **6** with high selectivity. In contrast, the homogeneous organometallic complex is very selective for the C=C bond hydrogenation to give **3**, especially under mild conditions. The higher activity of Ru@[C_{12}MIM][BTA] for the hydrogenation of the heteroaromatic ring can be attributed to the fact that the reduction involved a surface reaction rather than a reaction at an isolated metal center. This is confirmed further by the results of a mercury poisoning test.[15] The hydrogenation activity of Ru@[C_{12}MIM][BTA] was quenched completely, and no further change in the product distribution was observed, when an excess of mercury was added to the reaction mixture after 1 h reaction time. In contrast, the hydrogenation with the molecular catalyst complex [RuHCl(PPh_3)$_3$] remained unaffected by the addition

of Hg and conversion continued as in the reference experiment. This is a strong indication that the hydrogenation of **2** is catalysed by ruthenium nanoparticles rather than by molecular species leaching into solution.[16] At high temperature and hydrogen pressure, Ru on alumina leads to **6** as the major product with even slightly higher selectivity than Ru@[C_{12}MIM][BTA]. At mild conditions, however, product **3** was largely favoured with only moderate amounts of **4** present in the product mixture. This indicates that Ru@[C_{12}MIM][BTA] is a considerably more active catalytic system for the hydrogenation of the heteroaromatic ring in substrate **2**. This distinct catalytic behaviour of Ru@[C_{12}MIM][BTA] complements the range of products that is obtained *via* hydrogenation of **2**. In particular, both substituted ketones and alcohols are accessible in high selectivities from furfuryl-based biogenic substrates.

Conclusion

The results of this study demonstrate that IL-stabilized Ru nanoparticles are effective catalysts for the selective hydrogenation of biomass based substrates. The activity, selectivity and stability of the nanoparticles can be influenced and controlled by variation of the ionic liquids. In particular, Ru@[C_{12}MIM][BTA] provides a promising catalytic system allowing hydrogenation of C=C, C=O, arenes and heteroaromatic systems with a distinct selectivity and reactivity towards the different functional groups. The catalytic performance is complementary to both classical homogeneous and heterogeneous catalysts. Recycling of the catalyst by $scCO_2$ extraction of the products is possible without significant loss in selectivity and reactivity.

Experimental

General

All reactions involving air-sensitive materials were carried out under argon atmosphere using standard Schlenk techniques. The ionic liquids 1-ethyl-3-methylimidazolium bromide, 1-ethyl-2,3-dimethylimidazolium bis(trifluoromethylsulfonyl)-imide and 1-ethyl-3-methylimidazolium bis(trifluoromethylsulfonyl)imide were prepared according to known procedures.[17] Their purity was checked by ^{1}H-/^{13}C-NMR spectra and the water content was determined by Karl-Fischer titration. 4-(5-Hydroxymethyl-2-furyl)-3-butene-2-one **2** was synthesized by a modified aldol condensation of 5-hydroxymethylfurfural and acetone.[18] All other chemicals were purchased from commercial sources and used without further purification. NMR spectra were recorded on a Bruker AV400 spectrometer. Gas chromatography analysis was performed with a Siemens Sichromat 1–4 gas chromatograph with FID detector and a 60 m capillary column with a polyethyleneglycol stationary phase. Mass spectra were obtained using a MAT 5 Thermo Finigan (EI, 70 eV). X-Ray diffraction (XRD) analysis was performed using a Siemens D5000 X-ray diffractometer operating at 40 kV and 40 mA with Cu K_α radiation. Transmission electron microscopy (TEM) was performed on a Hitachi-HF-200 operating at 200 kV at the MPI Mülheim. Inductively-coupled-plasma mass spectra (ICP-MS) were measured at the microanalytical laboratory by H. Kolbe in Mülheim.

Synthesis of 4-(5-hydroxymethyl-2-furyl)-3-butene-2-one (1)

4-(5-Hydoxymethyl-2-furly)-3-butene-2-one **1** was synthesized by aldol condensation of 5-hydroxymethylfurfural and acetone. 5-Hydroxymethylfurfural (2.00 g; 15.89 mmol) was dissolved in 10 equivalents (11.6 mL, 158.90 mmol) of acetone and 0.1 mL of 0.1 M NaOH. The reaction mixture was stirred at room temperature for 12 h. After removal of the solvent under reduced pressure, the yellow residue was solved in H_2O and washed with ethyl acetate until the aqueous phase was colourless. The organic phases were combined and the solvent was removed under reduced pressure. The residue was purified by column chromatography (silica gel, pentane-ethyl acetate 1 : 2) to give **1** (1.87 g, 71%) as a pale yellow powder.

Preparation and characterization of transition-metal nanoparticles

Transition-metal nanoparticles were prepared by chemical reduction of bis(methylallyl)(1,5-cyclooctadiene)ruthenium(II) with hydrogen. In a typical experiment the precursor (5.1 mg; 0.016 mmol) was dispersed in ionic liquid (62.0 mg) and the reaction mixture was placed in a 10 mL stainless-steel high pressure reactor with a glass inlet, which was pressurized to 60 bar with H_2 and heated to 60 °C. After stirring for 2 h, the reactor was cooled to ambient temperature and carefully vented. A dark brown solution was obtained that was used directly for the hydrogenation reaction.

The morphology of Ru nanoparticles before and after catalysis was analysed *via* TEM. The samples were prepared by dilution of the nanoparticle solution with acetone and deposition on a carbon coated copper grid. For XRD analysis the nanoparticles were separated from the dark brown solution by adding acetone and centrifuging the mixture (5000 rpm, 25 min). A black powder could be isolated, which was washed two times with acetone and dried under reduced pressure.

Catalytic hydrogenation

All hydrogenation reactions were carried out in a 10 mL stainless-steel high pressure reactor with a glass inlet. To the solution of nanoparticles in the IL 4-(2-furyl)-3-butene-2-one (**2**; 217.8 mg; 1.60 mmol) was added (ruthenium/substrate ratio: 1 : 100). The reactor was pressurized to 120 bar with hydrogen and heated to 120 °C. After stirring for 2 h, the reactor was cooled to ambient temperature and carefully vented. For GC and NMR analysis the reaction mixture was filtered over silica with pentane/ether 1 : 2. The obtained colourless to pale yellow solution was concentrated under reduced pressure. The hydrogenation reaction with 5% ruthenium on alumina or $RuHCl(PPh_3)_3$ as catalysts was carried our under the same conditions in presence of IL.

Monitoring the course of reaction

To monitor the hydrogenation of **2**, the reaction was carried out in a 100 mL stainless-steel high pressure reactor with a sampling device. The volume of each sample was 0.15 mL. To guarantee a sufficient volume for sampling the standard reaction solution was scaled-up to a total amount of 10 mL. The reactor was heated to 60 °C and pressurized to 60 bar with hydrogen.

The pressure was kept constant during the monitoring by an external hydrogen reservoir. To monitor the hydrogenation of acetophenone, the same conditions and ruthenium/substrate ratios were applied.

Hg poisoning test

Hg poisoning tests were carried out using the same standard hydrogenation conditions. Bis(methylallyl)(1,5-cyclooctadiene)ruthenium(II) (5.1 mg; 0.016 mmol) was dispersed in [C_{12}MIM][BTA] (62.0 mg; 0.117 mmol). After stirring for 2 h at 60 °C and 60 bar H_2 pressure **2** (217.8 mg, 1.60 mmol) was added. The reactor was pressurized to 120 bar hydrogen and heated to 120 °C. After 1 h reaction time, the reaction was cooled down to ambient temperature and carefully vented. A small sample was collected to be analyzed by GC. Elemental Hg (1.355 g, 422 equiv.) was added to the reaction mixture. After stirring for 10 h, the reaction mixture was heated to 120 °C and pressurized to 120 bar with hydrogen for 1 h. Afterwards the reactor was cooled down, depressurized and a sample was taken for GC analysis. The Hg poisoning reaction with $RuHCl(PPh_3)_3$ as catalyst was carried out under the same conditions.

Recycling

For recycling, the products were extracted with $scCO_2$ from the reaction mixture after the reaction. The extraction was carried out at 40 °C and 150 bar CO_2 pressure for 3 h with an average flow rate of 287.5 mL min^{-1} under continuous conditions. The extract was collected in a cooling trap kept at –45 °C in a 2-propanol/dry ice bath.

Acknowledgements

This work was supported by the Deutsche Bundesstiftung Umwelt (DBU) and in part by the Cluster of Excellence "Tailor-Made Fuels from Biomass" (TMFB), which is funded by the Excellence Initiative of the German federal and state governments to promote science and research at German universities. TEM measurements by B. Spliethoff (MPI für Kohleforschung, Mülheim/Ruhr) are gratefully acknowledged.

Notes and references

1 (*a*) G. W. Huber, S. Iborra and A. Corma, *Chem. Rev.*, 2006, **106**, 4044; (*b*) A. Corma, S. Iborra and A. Velty, *Chem. Rev.*, 2007, **107**, 2411; (*c*) F. M. A. Geilen, B. Engendahl, A. Harwardt, W. Marquardt, J. Klankermayer and W. Leitner, *Angew. Chem. Int. Ed.*, 2010, **49**, 5510; (*d*) R. Palkovits, *Angew. Chem. Int. Ed.*, 2010, **49**, 4336.
2 (*a*) K. Lourvanij and G. L. Rorrer, *Ind. Eng. Chem. Res.*, 1993, **32**, 11; (*b*) C. Moreau, R. Durand, D. Peyron, J. Duhamet and P. Rivalier, *Ind. Crops Prod.*, 1998, **7**, 95.
3 (*a*) G. W. Huber, J. N. Chheda, C. J. Barrett and J. A. Dumesic, *Science*, 2005, **308**, 1446; (*b*) C. J. Barrett, J. N. Chedda, G. W. Huber and J. A. Dumesic, *Appl. Catal., B*, 2006, **66**, 111.
4 M. Chatterjee, K. Matsushima, Y. Ikushima, M. Sato, T. Yokoyama, H. Kawanami and T. Suzuki, *Green Chem.*, 2010, **12**, 779.
5 (*a*) J. Dupont and J. D. Scholten, *Chem. Soc. Rev.*, 2010, **39**, 1780; (*b*) D. Astruc, *Nanoparticles and Catalysis*, 2008, WILEY-VCH, Weinheim; (*c*) D. Astruc, F. Lu and J. R. Aranzaes, *Angew. Chem.*, 2005, **117**, 8062; D. Astruc, F. Lu and J. R. Aranzaes, *Angew. Chem., Int. Ed.*, 2005, **44**, 7852.
6 (*a*) J. Dupont, G. S. Fonseca, A. P. Umpierre, P. F. P. Fichtner and S. R. Teixeira, *J. Am. Chem. Soc.*, 2002, **124**, 4228; (*b*) A. P. Fonseca, P. F. P. Umpierre Fichtner, S. R. Teixeira and J. Dupont, *Chem.–Eur. J.*, 2003, **9**, 3263; (*c*) M. H. G. Prechtl, M. Scariot, J. D. Scholten, G. Machado, S. R. Teixeira and J. Dupont, *Inorg. Chem.*, 2008, **47**, 8995.
7 V. Cimpeanu, M. Kočevar, V. I. Parvulescu and W. Leitner, *Angew. Chem.*, 2009, **121**, 1105; V. Cimpeanu, M. Kočevar, V. I. Parvulescu and W. Leitner, *Angew. Chem., Int. Ed.*, 2009, **48**, 1085.
8 J. D. Aiken and R. G. Finke, *J. Mol. Catal. A: Chem.*, 1999, **145**, 1.
9 (*a*) H. Bönnemann and R. M. Richards, *Eur. J. Inorg. Chem.*, 2001, 2455; (*b*) G. Schmid, *Chem. Rev.*, 1992, **92**, 1709; (*c*) G. Schmid (Ed.), *Nanotechnology*, 2008, WILEY-VCH, Weinheim.
10 M. Antonietti, D. B. Kuang, B. Smarsly and Y. Zhou, *Angew. Chem.*, 2004, **116**, 5096; M. Antonietti, D. B. Kuang, B. Smarsly and Y. Zhou, *Angew. Chem., Int. Ed.*, 2004, **43**, 4988.
11 L. S. Ott, M. L. Cline, M. Deetlefs, K. R. Seddon and R. G. Finke, *J. Am. Chem. Soc.*, 2005, **127**, 5758.
12 E. T Silveira, A. P. Umpierre, L. M. Rossi, G. Machado, J. Morais, G. V. Soares, I. J. R. Baumvol, S. R. Teixeira, P. F. P. Fichtner and J. Dupont, *Chem.–Eur. J.*, 2004, **10**, 3734.
13 (*a*) P. G. Jessop, W. Leitner, *Chemical Synthesis Using Supercritical Fluids*, 2nd Edition, 2010, WILEY-VCH, Weinheim; (*b*) J. Langanke and W. Leitner, *Top. Organomet. Chem.*, 2008, **23**, 91; (*c*) D. J. Cole-Hamilton, *Science*, 2003, **299**, 1702.
14 G. S. Fonseca, J. D. Scholten and J. Dupont, *Synlett*, 2004, 1525.
15 J. A. Widegren and R. G. Finke, *J. Mol. Catal. A: Chem.*, 2003, **198**, 317.
16 (*a*) C. C. Cassol, A. P. Umpierre, G. Machado, S. I. Wolke and J. Dupont, *J. Am. Chem. Soc.*, 2005, **127**, 3298; (*b*) J. G. de Vries, *Dalton Trans.*, 2006, 421; (*c*) L. D. Pachón and G. Rothenberg, *Appl. Organomet. Chem.*, 2008, **22**, 288.
17 (*a*) J. D. Holbrey, W. M. Reichert, R. P. Swatloski, G. A. Broker, W. R. Pitner, K. R. Seddon and R. D. Rogers, *Green Chem.*, 2002, **4**, 407; (*b*) J. S. Wilkes, J. A. Levisky, R. A. Wilson and C. L. Hussey, *Inorg. Chem.*, 1982, **21**, 1263.
18 H. Quiroz-Florentino, R. Aguilar, B. M. Santoyo, F. Díaz and J. Tamariz, *Synthesis*, 2008, **7**, 1023.